ICAS 2021 SHANGHAI
International Council of the Aeronautical Sciences
32nd Congress of the International Council of the Aeronautical Sciences
September 6-10, 2021
Pudong Shangri-La, Shanghai, China

ADRC Based High Maneuvering Flight Control Law Design for UAV

ZHOU Wangyi[1], He Shaomin[1], Tian Mingming[1]

[1] AVIC Xi'an Flight Automatic Control Research Institute, Xi'an, China, 710065

Abstract

Unmanned aerial vehicle (UAV) requires to maximize its maneuverability and has the control ability of high maneuvering flight in the process of attacking, escaping, and avoiding enemy weapon attacks in air combat to improve the survival probability. Aiming at the problems of aerodynamic coupling, strong nonlinearity and strong disturbance in the high maneuvering flight of UAV, a comprehensive high maneuvering flight control law with longitudinal, lateral, directional and speed multi control channels is designed based on the auto disturbance rejection controller (ADRC). The ADRCs of all control modes are composed of a third-order extended state observer (ESO), a second-order tracking differentiator (TD), and nonlinear state error feedback (NLSEF), which can realize the real-time estimation and compensation of disturbances from the inside and outside of the control system, so as to ensure the stability of UAV in the entire maneuvering flight. The effectiveness and reliability of the designed ADRC control law are verified by Kulbit maneuver control considering the deviation of aerodynamics. Through comparing with the classical PID control method, it is confirmed that the ADRC can effectively resist the internal and external interferences, maintain the response quality, and ensure robustness of the control system.

Keywords: Auto Disturbance Rejection Controller; Extended State Observer, High Maneuvering Flight Control

1. General Introduction

There are following three notable characteristics in the high maneuvering flight process of UAVs: First, the flight status and nonlinear aerodynamics changes drastically when facing with deformation of configuration and large overload maneuver; second, the atmospheric turbulence, wind disturbance and aerodynamic deviation seriously affect the dynamic and static control performance in high maneuvering flight; third, the control parameters involve overload, attitude angle, speed and position, it is difficult for a single control mode to meet the precise control requirements of high maneuverability. It is hard to establish an accurate plane model due to above characteristics, and the classic control technology is unable to support the combat mission, a highly robust nonlinear control algorithm to reduce the impact of undesirable characteristics on the closed-loop control performance is indispensable [1, 2].

In order to overcome the nonlinear coupling characteristics and the influence of uncertainty in maneuvering flight, literature [3, 4] adopted a high-order sliding mode control method to design flight control law, and decomposed complex maneuver into several stages for targeted control design. Literature [5] used full-state feedback to offset the nonlinear term and realized the flight control of multiple maneuvers. Literature [6] combined adaptive control and neural network algorithm to design a smart missile maneuvering controller. The above methods have high requirements on the operational capability of the flight control computer, which may be not conducive to engineering realization.

The ADRC is a relatively simple but effective method that can solve the control problems of large-scale and complex uncertain systems. ADRC does not rely on the exact model of controlled system, and can directly utilize the input and output signals of the controlled object to estimate and compensate the system state and total disturbance. It still maintains good control performance when there exists multiple uncertainties, with the advantages of high precision, high anti-interference and strong robustness [7, 8].

Aiming at various application scenarios and control demands of high maneuvering flight, this paper

designs the control law of all flight modes based on ADRC, and conducts simulations under the disturbance of aerodynamic coefficients and sensor inputs, and finally realizes Kulbit maneuver control. All the simulations verify that the ADRC is suitable for the for high maneuvering flight control under strong nonlinear and disturbing environment.

2. Six degrees of freedom plane model

The controlled UAV is a conventional layout, with control surfaces of elevator, aileron and rudder. Regardless of the rotation of the earth and the aeroelastic deformation of the UAV, the dynamic equations of aircraft motion can be described by the following twelve first-order differential equations:

$$\dot{u} = vr - wq - g\sin\theta + \frac{F_x}{m} \tag{1}$$

$$\dot{v} = -ur + wp + g\cos\theta\sin\phi + \frac{F_y}{m} \tag{2}$$

$$\dot{w} = uq - vp + g\cos\theta\cos\phi + \frac{F_z}{m} \tag{3}$$

$$\dot{\phi} = p + (r\cos\phi + q\sin\phi)\tan\theta \tag{4}$$

$$\dot{\theta} = q\cos\phi - r\sin\phi \tag{5}$$

$$\dot{\psi} = \frac{1}{\cos\theta}(r\cos\phi + q\sin\phi) \tag{6}$$

$$\dot{p} = (c_1 r + c_2 p)q + c_3 L + c_4 N \tag{7}$$

$$\dot{q} = c_5 pr - c_6(p^2 - r^2)q + c_7 M \tag{8}$$

$$\dot{r} = (c_8 p - c_2 r)q + c_4 L + c_9 N \tag{9}$$

$$\dot{x}_g = u\cos\theta\cos\psi + v(\sin\phi\sin\theta\cos\psi - \cos\phi\sin\psi) + w(\sin\phi\sin\psi + \cos\phi\sin\theta\cos\psi) \tag{10}$$

$$\dot{y}_g = u\cos\theta\sin\psi + v(\sin\phi\sin\theta\sin\psi + \cos\phi\cos\psi) + w(-\sin\phi\cos\psi + \cos\phi\sin\theta\sin\psi) \tag{11}$$

$$\dot{h} = u\sin\theta - v\sin\phi\cos\theta - w\cos\phi\cos\theta \tag{12}$$

In the formula, $c_1 = \frac{(I_y - I_z)I_z - I_{xz}^2}{\sum}$, $c_2 = \frac{(I_x - I_y + I_z)I_{xz}}{\sum}$, $c_3 = \frac{I_z}{\sum}$, $c_4 = \frac{I_{xz}}{\sum}$, $c_5 = \frac{I_z - I_x}{I_y}$, $c_6 = \frac{I_{xz}}{I_y}$, $c_7 = \frac{1}{I_y}$, $c_8 = \frac{I_x(I_x - I_y) + I_{xz}^2}{\sum}$, $c_9 = \frac{I_x}{\sum}$, $\sum = I_x I_z - I_{xz}^2$. Where u, v, w represents the three-axis speed; ϕ, θ, ψ stands for the roll angle, pitch angle and heading angle; p, q, r represents the three-axis angular rate; x_g, y_g, h represents the ground displacement; F_x, F_y, F_z represents the three-axis force; L, M, N represents the three-axis torque. The high-maneuvering flight control law is designed based on the above-mentioned nonlinear six degree of freedom plane model.

3. Design of High Maneuvering Flight Control Law

3.1 Principle and structure of ADRC method

Suppose an uncertain object with unknown disturbance as:

$$x^{(n)} = f(x, \dot{x}, \cdots, x^{(n-1)}, t) + w(t) + bu(t) \tag{13}$$

In the formula, $f(\cdot)$ is an uncertain function, $u(t)$ is the input, and $w(t)$ is the unknown external disturbance term. Select the state variables as $[x_1, x_2, \cdots, x_n]^{\mathrm{T}} = [x, \dot{x}, \cdots, x^{(n-1)}]^{\mathrm{T}}$, and construct the extended state variables, then the extended state equation of the system is expressed as follows:

$$\begin{cases} \dot{x}_1 = x_2 \\ \vdots \\ \dot{x}_{n-1} = x_n \\ \dot{x}_n = x_{n+1} + bu \\ \dot{x}_{n+1} = \dot{a}(t) \\ y = x_1 \end{cases} \tag{14}$$

Construct the extended state observer as:

$$\begin{cases} \dot{z}_1 = z_2 - \beta_1 g_1(z_1 - y) \\ \vdots \\ \dot{z}_n = z_{n+1} - \beta_n g_n(z_1 - y) + bu \\ \dot{z}_{n+1} = -\beta_{n+1} g_{n+1}(z_1 - y) \end{cases} \tag{15}$$

In the formula, β_k is a constant coefficient; g_k is a nonlinear function. z_{n+1} is the feedback control variable, recording as $u = -z_{n+1}/b_0 + u_0$, and the system is transformed into integrator-series type, where $-z_{n+1}/b_0$ is the compensation for the total disturbance of the system, and u_0 is the combination of the nonlinear error signal $e_1, e_2, \cdots, e_n$.

The second-order tracking differentiator provides the tracking signal v_1 and its differential signal v_2 of the given command signal y_c, and the structure is denoted as follow:

$$\begin{cases} \dot{v}_1 = v_2 \\ \dot{v}_2 = -rsat(v_1 - y_c + v_2|v_2|/(2r), \delta) \end{cases} \tag{16}$$

The expression of the linear saturation function is:

$$sat(x, \delta) = \begin{cases} sign(x), |x| \geq \delta \\ x/\delta, |x| < \delta \end{cases} \tag{17}$$

The NLSEF combines the tracking signal and its differential signal with the error of the state estimator nonlinearly, in the form:

$$u_0 = \sum_{i=1}^{n} K_i \, fal(e_i, \alpha_i, \delta_i) \tag{18}$$

Where

$$fal(e, \alpha, \delta) = \begin{cases} |e|^{\alpha} \, sign(e), |e| \geq \delta \\ e/\delta^{1-\alpha}, \quad |e| < \delta \end{cases} \tag{19}$$

After adding the compensation to the total disturbance, the control input of the controlled object is generated as $u(k) = u_0 - z_3(k)/b_0$.

The structure of the second-order ADRC applied in this article is shown in Figure 1, consisting of the TD, NLSEF and ESO mentioned above.

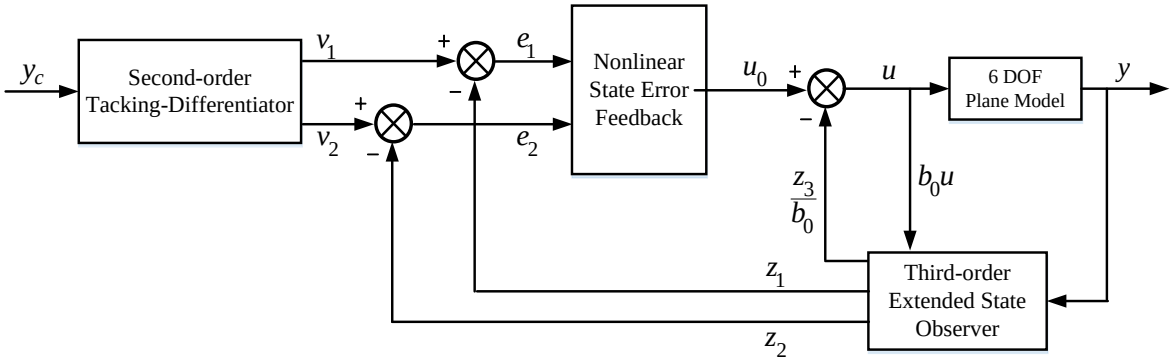

Figure 1 – Structure diagram of second-order ADRC.

3.2 ADRC design of longitudinal, lateral, directional and speed control channels

Maneuver can be regarded as an orderly execution process of a set of instructions. A series of standard maneuvers are formed according to tactical decisions, which are further decomposed to form the underlying requirements for the control law. Combined with the application characteristics of the ADRC algorithm, the longitudinal, lateral, directional and speed control channels are designed based on the nonlinear six degree of freedom plane model. The nonlinear dynamics of the UAV is divided into the fast inner-loop variables and the slow outer-loop variables. The multi-channel control structure with inner and outer loop integrated based on ADRC is shown in Figure 2. All control modes are designed on the basis of the second-order ADRC controller described in the previous section. The inner loop of the longitudinal channel is the normal acceleration control mode, which sequentially nests the pitch angle hold mode, vertical speed control mode and altitude hold mode. The inner loop of lateral and directional channel is roll angle rate control mode, and the outer loop is roll angle hold mode and heading angle hold mode successively. Sideslip angle and yaw rate feedback are introduced to enhance the lateral and directional stability. The speed control mode is a closed-loop control with indicated airspeed command as input and throttle percentage as output. Taking the coupling and nonlinearity of each channel and the external disturbances as the total disturbances of the system model, the ADRC can estimate and compensate these perturbations in real time to realize the decoupling design of each control channel.

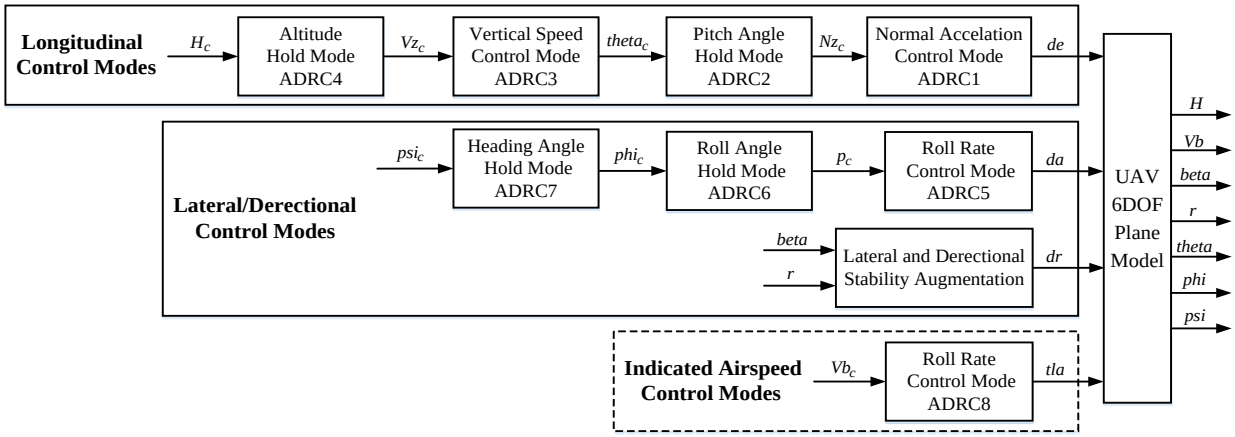

Figure 2 – Structure diagram of control modes for longitudinal, lateral, directional and speed channels.

In ESO, the nonlinear coefficient is related to the bandwidth ω, $\beta_1 = 3\omega, \beta_2 = 3\omega^2$, $\beta_2 = \omega^3$. The bandwidth of inner loop control mode is taken as 5. The bandwidth of the outer loop control mode is taken as 0.5, which is much smaller than the inner loop. b_0 is the only parameter concerned with the controlled object, which plays an important role in the performance of ADRC, and can be adjusted adaptively according to flight status and disturbing situation. The parameters of the TD are related to the tracking speed and noise filtering effect. The coefficients of NLSEF are related to the requirement of system response speed.

4. Simulation verification

Based on the nonlinear six degree of freedom plane model and the designed controller, a simulation model is established to verify the feasibility and practicability of the ADRC algorithm applied to high maneuvering flight control from the following three aspects.

4.1 Simulation of Comparison between ADRC and PID algorithm

The flight condition of the simulation is set at 3000m in altitude and 0.4 in Mach number. The normal acceleration control command for the longitudinal inner loop is a 4G step command, and the roll angle rate control command for the lateral and directional inner loop is a 100°/s step command. Compare the inner loop control effect of ADRC and PID algorithm: First, design the inner loop controller based on PID so that the response of PID control is as consistent as possible with ADRC control under the same flight condition and control instructions without any disturbances, shown in Figure 3(a) and Figure 4(a); then, set the aerodynamic coefficients Fx, Fy, Fz and aerodynamic moment coefficients Mx, My, Mz as random white noise distribution, and the

maximum deviation of disturbance is 30% of the baseline value. Step instructions are given to the normal acceleration and roll angle rate control modes respectively, the simulation results are displayed in Figure 3(b) and Figure 4(b); finally, the normal overload sensor and roll angle rate sensor are set as the random white noise distribution, and the maximum deviation of disturbance is 15% of the reference value. After instructing step commands, the simulation results are demonstrated in Figure 3(c) and Figure 4(c). It can be seen from the figures that when random disturbances are added, the normal acceleration and roll angle rate still fluctuate after the responses reach to steady state, and even high-frequency oscillation occurs considering the sensor disturbance under PID control. However, the response curves under ADRC control are stable and without steady-state error. With the random disturbance of the sensor, the transient response performance of the roll angle rate controlled by ADRC is also significantly better than PID control, and its the rise time is basically the same as that without disturbance. Compared with the traditional PID algorithm, it concludes that ADRC algorithm possesses filtering characteristics and remarkable anti-interference ability against disturbances from the inner aerodynamic coefficients and the outer sensors of the control system.

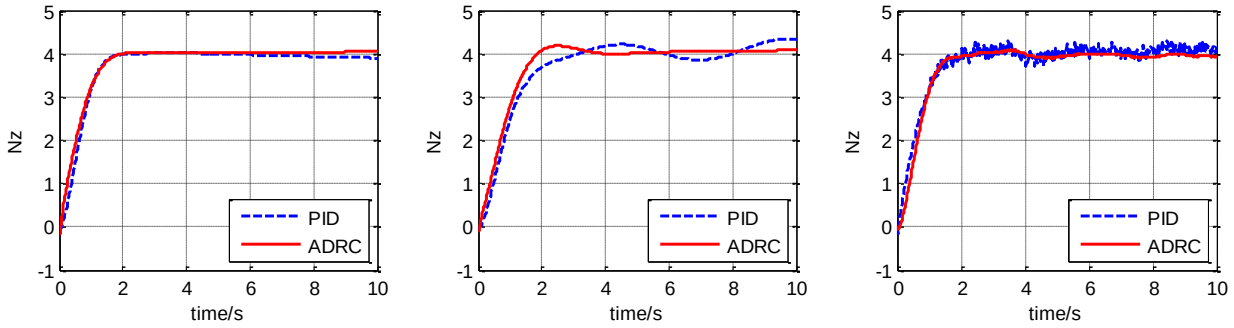

(a) No disturbance (b) 30% aerodynamic coefficient random disturbance (c) 15% normal overload tensor random disturbance

Figure 3 – ARDC and PID comparison of normal acceleration control mode.

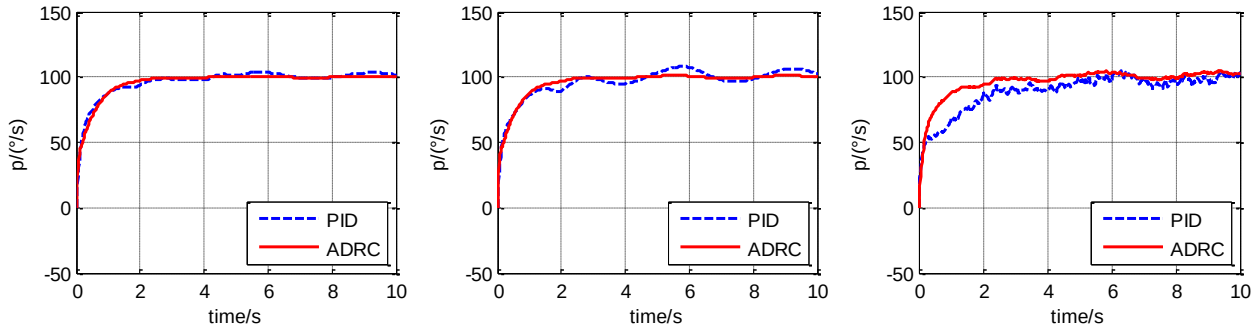

(a) No disturbance (b) 30% aerodynamic coefficient random disturbance (c) 15% normal overload tensor random disturbance

Figure 4 – ARDC and PID comparison of roll rate control mode.

4.2 Simulation of ADRC control modes in different flight conditions

In order to verify that all control modes designed based on the ADRC have a good control effect in the flight envelope, a total of 12 flight conditions as shown in Table 1 are selected for simulation.

Table 1 – Twelve flight conditions selected for simulation of ADRC control modes.

Flight condition	Altitude/m	Mach number
1	1000	0.2
2	1000	0.4
3	1000	0.6
4	2000	0.2
5	2000	0.4
6	2000	0.7
7	4000	0.4
8	4000	0.6

9	4000	0.8
10	6000	0.6
11	6000	0.7
12	6000	0.9

Based on the plane trim values of the 12 flight conditions, incremental step commands are instructed to the eight designed control modes respectively. For simulations of longitudinal control modes, set 7g normal acceleration, 10° pitch angle, 10m/s vertical speed, and 100m altitude incremental commands in sequence. The roll angle remains at 0° and the indicated speed remains at the current trim value simultaneously. For simulation lateral and directional control modes, set the 100°/s roll angle rate, 60° roll angle, and 10° heading angle incremental commands sequentially. At the same time, the altitude and the indicated speed are controlled to the current trim values. For simulation of speed control mode, set the 10m/s indicated speed incremental command, and the altitude maintains at the current trim value, and the roll angle keeps at 0°. From the simulation curves shown in Figure 5, it is proved that all control modes have excellent dynamic characteristics in different flight states, and the steady-state values are basically within 5% error range, indicating that the designed control law has favorable robustness. The rise time of the normal acceleration and the roll angle rate control modes is about 1s, which can quickly track and respond to control commands in order to meet the agility performance of high maneuvering flight.

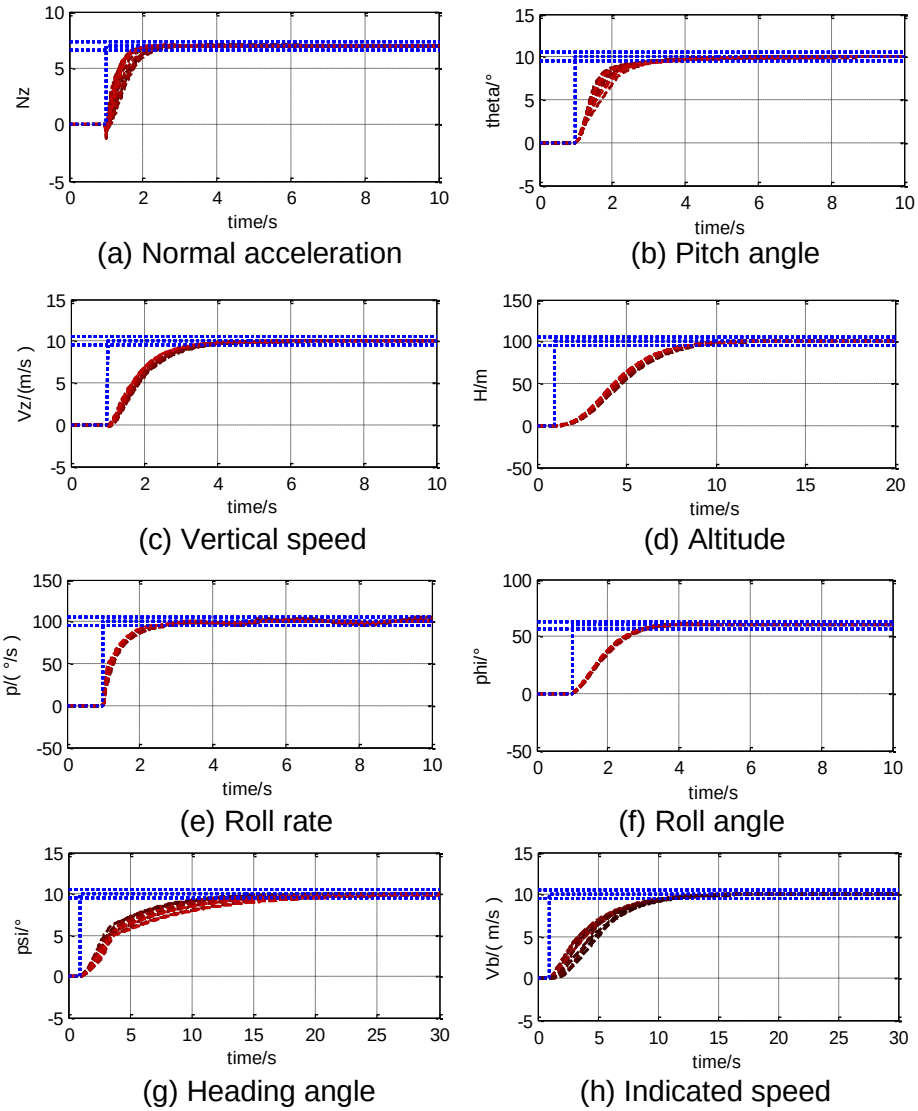

(a) Normal acceleration (b) Pitch angle

(c) Vertical speed (d) Altitude

(e) Roll rate (f) Roll angle

(g) Heading angle (h) Indicated speed

Figure 5 – Simulations of designed ARDC control modes in different flight conditions.

4.3 Simulation of Kulbit Maneuver control

The Kulbit Maneuver is a quite lethal defensive maneuver, which can make the UAV suddenly change the direction of flight to attack the enemy aircraft in the tail. Based on the ADRC method,

the simulation of Kulbit Maneuver control is established. Combining the demands for the guidance law, the corresponding altitude command, normal acceleration command, pitch angle command, and indicated speed command are given at different stages of the Kulbit Maneuver. The initial state of the UAV is chosen at the 3000m altitude and 0.7 Mach number, and the radius of Kulbit Maneuver is 600m. The combination of aerodynamic coefficients and aircraft mass is deviated by 10% from the reference values to simulate the inaccuracy of the plane model in real flight. The trajectory of the Kulbit maneuver is displayed in Figure 6, and flight state variables during the maneuver is shown in Figure 7. In the condition of disturbing effects, the deviation of completion time is controlled within 1s, the deviation of the angle of attack is less than 1.6°, and the overall height difference of the maneuver is controlled within 20m compared with the simulations of baseline plane model, which verifies that ADRC can estimate and compensate the uncertainty of the control system caused by aerodynamic and mass perturbation, and track the control command quickly and accurately, ensure the strong robustness of control system.

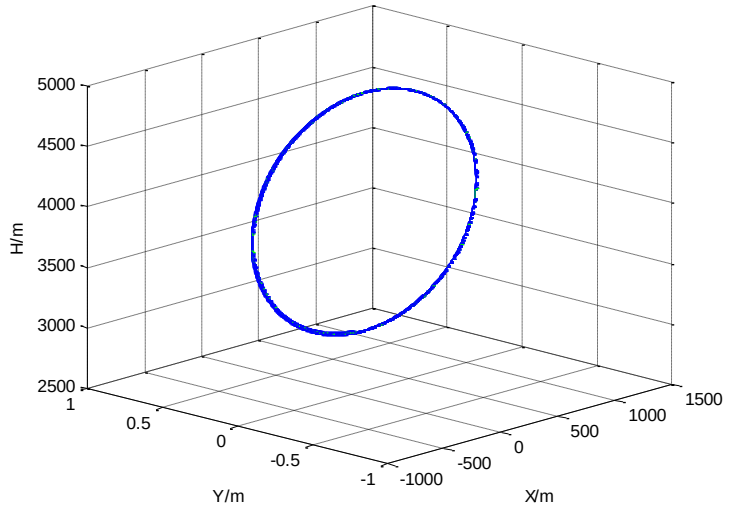

Figure 6 – The three-dimensional trajectory of the Kulbit maneuver simulation

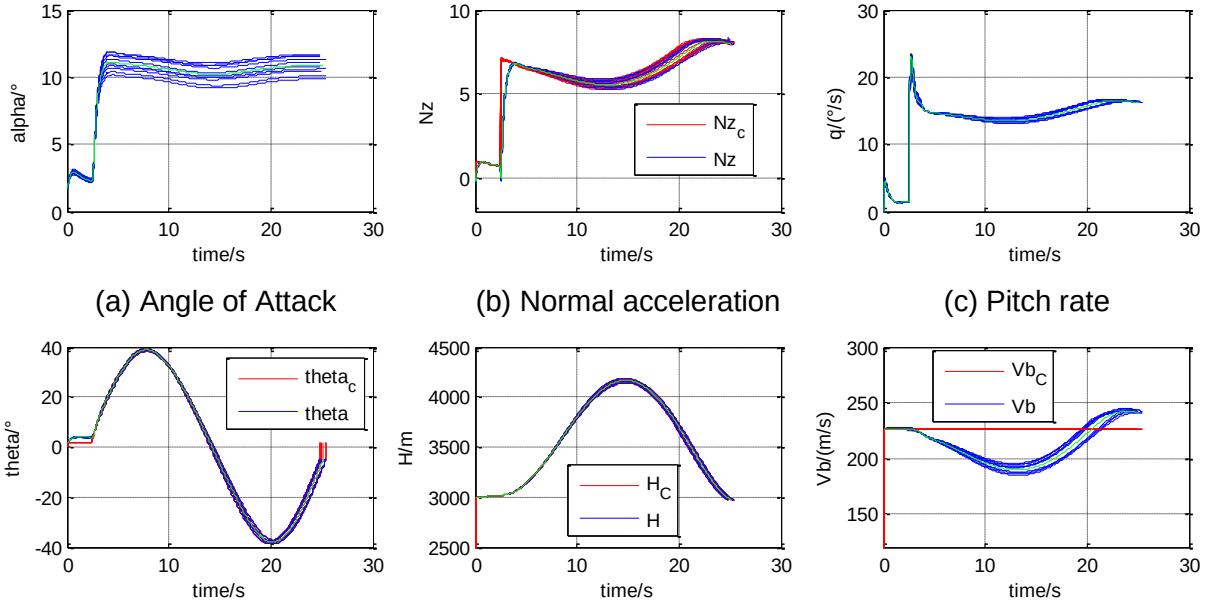

(a) Angle of Attack (b) Normal acceleration (c) Pitch rate

(d) Pitch angle (e) Altitude (f) Indicated speed

Figure 7 – The flight state variables of the Kulbit maneuver simulation

5. Conclusion

In this paper, a conventional layout UAV is chosen as the research object. Based on the nonlinear plane model, the high maneuvering flight control laws based on ADRC for longitudinal, lateral, directional and speed control modes are designed. The ADRC control law design does not require an accurate model of the controlled object, and can estimate and compensate for internal and

external disturbances and the coupling of different control channels to ensure the ideal dynamic and steady-state performance of the closed-loop system. The simulation of Kulbit maneuver is finally realized considering the deviation of aerodynamic coefficients and sensor input, which proves that the designed control law has strong anti-interference and robustness within the envelope range and provides a new way to solve the problem of maneuvering flight control.

6. Copyright Statement

References

[1] Schneider W. Defense science board study on unmanned aerial vehicles and uninhabited combat aerial vehicle. EB/OL, 2018.

[2] Alcorn C W, Croom M A, Francis M S. The X-31 aircraft: advances in aircraft agility and performance. Progress Aerospace Sciences, Vol. 32, No. 11, pp 377-413, 1996.

[3] Ure N K, Inalhan G. Autonomous control of unmanned combat air vehicles: design of a multimodal control and flight planning framework for agile maneuvering. IEEE Control Systems Magazine, Vol. 32, No. 5, pp 74-95, 2012.

[4] Ure N K, Inalhan G. Design of higher order sliding mode control laws for multimodal agile maneuvering UCAV. The 2nd International Symposium on Systems & Control in Aerospace & Astronautics, pp453-458, 2008.

[5] Snell S A, Nns d F, Arrard W L. Nonlinear inversion flight control for a super-maneuverable aircraft. Journal of Guidance Control and Dynamics, Vol. 15, No. 4, pp 976-984, 1992.

[6] Mcfarland M, Calise A J. Neural-adaptive nonlinear autopilot design for an agile anti-air missile. AIAA Guidance Navigation and Control Conference, pp 956-966, 1996.

[7] Han Jingqing. The auto disturbance rejection controller and its application. Control and Decision, Vol. 13, No. 1, pp 19-23, 1998.

[8] Han Jingqing. From PID technology to auto disturbance rejection control technology. Control Engineering, Vol. 9, No. 3, pp 13-18, 2002.